

図5 T細胞を利用したがん治療法

2. CTL療法とTIL療法

がん治療のためのワクチン療法については、60年以上もの研究が行われているにもかかわらず、治療法として浸透しているわけではない。患者の白血球を利用する治療法のCTL(cytotoxic T-lymphocyte)療法は、がんの治療に採り入れられている手法である(図5)。これは、患者の血液から分離したリンパ球のうち、キラーT細胞とよばれる細胞分画を、培養系で増幅するとともに、患者のがん細胞を標的とするように教育したのち、患者の血液に移植する方法である。この方法は、特異性の高い攻撃により、殺傷力は強い。

しかし、一つのT細胞は1種類のがん細胞抗原部位しか記憶することができない。さらに、患者の体内で転移したがん細胞は転移先の組織で抗原を変化させる。CTL療法の最大の問題点は、がん細胞の組織転移時に起こる抗原の変化に対応できないことにある。このCTL療法の短所を改善する試みも盛んに研究されており、T細胞の利用に加え、ワクチン療法を組み合わせる手法が開発されつつある。

類似の手法として、腫瘍組織浸潤リンパ球

(TIL : tumor-infiltrating lymphocyte)療法がある(図5)。腫瘍組織から分離したリンパ球を、インターロイキン2などのリンフォカインで増殖させて、活性化させたあとに患者に再移植する手法であり、CTL療法と並んで期待されている細胞移植療法である。

3. 細胞移植による再生医療

血球をつくる主な場所は骨髄である。骨髄には造血幹細胞(HSC : hematopoietic stem cell)とよばれる、増殖能が高く、それぞれの血球への分化能を持つ細胞群が存在する⁹⁾。この細胞群を細胞表面抗原により分離し、培養して増殖させ、サイトカインなどの刺激因子により目的とする血球へ分化させたのち、患者の体内へ戻す試みが行われている。患者自身の造血幹細胞を利用することにより、他人の血液から分離した血球を利用する際の危険性を回避できるとともに、ドナーの不足も解消できる。

一方、体内を循環する血液(末梢血)に血管内皮前駆細胞(EPC : endothelial progenitor cell)が存在することが発見された¹⁰⁾。それまで、生体の微小血管形成には、血管を構成する血管内皮細胞が増殖して新た

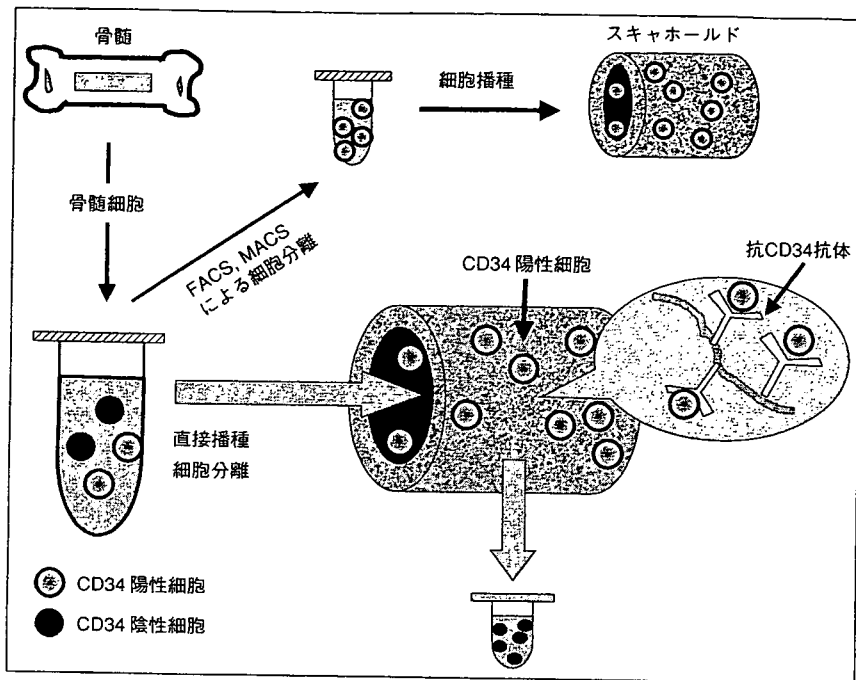


図6 幹細胞特異的吸着能を有する再生型人工血管スキャホールド

な血管を構築する，血管新生という概念が考えられてきたが，末梢血のEPCが発見されて以来，末梢血にあるEPCが血管を必要とする場所に集結・増殖して新たに血管を形成するという，発生時期のプロセスが成体でも認められるようになった．このEPCは，骨髓と末梢血に存在し，通常はほぼ平衡状態を保っているが，生体内の虚血部位で産生されるサイトカインや増殖因子などにより，骨髓から末梢血へリクルートされ，虚血部位での血管形成を誘導することがわかっている¹¹⁾．

近年，EPCに関連する研究が幅広く行われており，臨床の場での応用とその有用性が注目を集めている．まず，動物を用いた研究では，閉塞性動脈硬化症やバジュー病などの下肢虚血患者に対する治療，あるいは心筋虚血に対する治療として，自家EPC移植が試みられ，良好な結果が報告されている¹²⁾．それに伴い，最近では各国で臨床試験が行われるようになり，患者末梢血へのEPCの動因を向上させるための因子を投与したのち，EPCを採取して，患部に局所的にEPCを移植することにより，虚血部の血流回復が報告されている．

これらの血管再生能力を有する細胞群は，今後，再生医療で重要な役割を演じるであろう．1990年代より，骨髓細胞を播種した再生型人工血管の有用性

に関する研究結果が報告され¹³⁾，現在までに東京女子医科大学のグループが，骨髓細胞を利用した再生型人工血管の臨床応用を進めている¹⁴⁾．

筆者らの研究室では，ポリ乳酸(PLA)製のスキャホールドを利用した血管再生の研究を進めてきた．しかしながら，側鎖に官能基を持たないPLAなどの表面修飾反応は容易でないため，筆者らは，表面のみをアルカリで加水分解することでカルボキシル基を導入したあとに¹⁵⁾，幹細胞表面のCD34に対する抗体を固定化した．イヌ骨髓細胞をこの抗CD34固定化スキャホールドに播種したところ，効率よくCD34陽性細胞をトラップすることが明らかとなった(図6)．この機能性スキャホールドは，*in vivo*において，末梢血中のCD34陽性の機能細胞をリクルートすることで，速やかな血管組織への再構築を誘導できると期待して検討を重ねている．

おわりに

生涯にわたって，常に新しく産生されつづける血液の特徴を利用した新たな再生医療の展開が期待できる．人工赤血球や人工血小板など血液の代替材料の開発のみでなく，成分輸血など血液成分の利用，がんに対する血液中の免疫細胞の利用，さまざまな

組織の再生を目指した血液の細胞の利用など、新たな領域がつつぎと見いだされている。バイオマテリアル研究の血液との戦いが終結する気配はまったくない。

文 献

- 1) Bowman HW : Clinical evaluation of dextran as a plasma volume expander. J Am Med Assoc 1953, 153 : 24-26.
- 2) Sciqest 52 : 24, 1979.
- 3) Keipert PE, Chang TM : Pyridoxylated polyhemoglobin as a red cell substitute for resuscitation of lethal hemorrhagic shock in conscious rats. Biomater Med Devices Artif Organs 1985, 13 : 1-15.
- 4) 野上弥志郎, 木下 学, 高瀬凡平, 服部秀美, 庄野 聡・他 : 致死性出血性ショックに対する人工血液輸血の救命効果と生体に及ぼす影響. 人工臓器 2006, 35 : S-155.
- 5) Bode AP, Fischer TH : Lyophilized platelets : fifty years in the making. Artif Cells Blood Substit Immobil Biotechnol 2007, 35 : 125-133.
- 6) Teramura Y, Okamura Y, Takeoka S, Tsuchiyama H, Narumi H et al. : Hemostatic effects of polymerized albumin particles bearing rGPIa/IIa in thrombocytopenic mice. Biochem Biophys Res Commun 2003, 306 : 256-260.
- 7) Kim HW, GreenBurg AG : Toward 21st century blood component replacement therapeutics : artificial oxygen carriers, platelet substitutes, recombinant clotting factors, and others. Artif Cells Blood Substit Immobil Biotechnol 2006, 34 : 537-550.
- 8) Nakagawa M, Koyanagi M, Tanabe K, Takahashi K et al. : Generation of induced pluripotent stem cells without Myc from mouse and human fibroblasts. Nat Biotechnol 2007, Published on line Nov 30.
- 9) Yin AH, Miraglia S, Zanjani ED, Almeida-Porada G, Ogawa M et al. : AC133, a novel marker for human hematopoietic stem and progenitor cells. Blood 1997, 90 : 5002-5012.
- 10) Asahara T, Murohara T, Sullivan A, Silver M, van der Zee R et al. : Isolation of putative progenitor endothelial cells for angiogenesis. Science 1997, 275 : 964-967.
- 11) Asahara T, Masuda H, Takahashi T, Kalka C, Pastore C et al. : Bone marrow origin of endothelial progenitor cells responsible for postnatal vasculogenesis in physiological and pathological neovascularization. Circ Res 1999, 85 : 221-228.
- 12) Kawamoto A, Gwon HC, Iwaguro H, Yamaguchi JJ, Uchida S et al. : Therapeutic potential of *ex vivo* expanded endothelial progenitor cells for myocardial ischemia. Circulation 2001, 103 : 634-637.
- 13) 山岡哲二, 竹部義之, 木村良晴 : 高分子論文集 1998, 55 : 328-333.
- 14) Noishiki Y, Tomizawa Y, Yamane Y, Matsumoto A : Autocrine angiogenic vascular prosthesis with bone marrow transplantation. Nat Med 1996, 2 : 32-34.
- 15) Shin'oka T, Matsumura G, Hibino N, Naito Y, Watanabe M et al. : Midterm clinical result of tissue-engineered vascular autografts seeded with autologous bone marrow cells. J Thorac Cardiovasc Surg. 2005, 129 : 1330-1338.

Scaffolds from electrospun polyhydroxyalkanoate copolymers: Fabrication, characterization, bioabsorption and tissue response

Tang H. Ying^{a,b}, Daisuke Ishii^c, Atsushi Mahara^d, Sunao Murakami^d, Tetsuji Yamaoka^d, Kumar Sudesh^{a,b}, Razip Samian^b, Masahiro Fujita^{a,*}, Mizuo Maeda^a, Tadahisa Iwata^{c,**}

^a Bioengineering Laboratory, RIKEN Institute, 2-1 Hirosawa, Wako-shi, Saitama 351-0198, Japan

^b School of Biological Science, Universiti Sains Malaysia, 11800 Penang, Malaysia

^c Department of Biomaterial Sciences, Graduate School of Agricultural and Life Sciences, The University of Tokyo, 1-1-1 Yayoi, Bunkyo-ku, Tokyo 113-8657, Japan

^d Department of Biomedical Engineering, Advanced Medical Engineering Center, National Cardiovascular Center Research Institute, 5-7-1 Fujishirodai, Suita, Osaka 565-8565, Japan

Received 10 September 2007; accepted 24 November 2007

Available online 21 December 2007

Abstract

Polyhydroxyalkanoate (PHA) copolymers of poly[(*R*)-3-hydroxybutyrate-*co*-5mol%-(*R*)-3-hydroxyhexanoate], poly[(*R*)-3-hydroxybutyrate-*co*-7mol%-4-hydroxybutyrate] and poly[(*R*)-3-hydroxybutyrate-*co*-97mol%-4-hydroxybutyrate] were electrospun to fabricate scaffolds with enhanced biocompatibility and bioabsorption. Subcutaneous implantation of the fibers in rats was performed to investigate their bioabsorption behavior and tissue response. The fibers before and after the *in vivo* experiments were characterized using gel permeation chromatography, scanning electron microscopy, X-ray diffraction and tensile test. Histological evaluation was also performed to determine the tissue response. The structures and properties of the electrospun PHA copolymers were compared with those of the electrospun poly[(*R*)-3-hydroxybutyrate]. The content and type of the second monomer and the diameter of fiber significantly influence the bioabsorption. The tissue response was found to improve with the high content of 4-hydroxybutyrate.

© 2007 Elsevier Ltd. All rights reserved.

Keywords: Electrospun fiber; Polyhydroxyalkanoate; Tissue response; Bioabsorption

1. Introduction

In response to the growing demand in the field of tissue engineering, the number of polyhydroxyalkanoates (PHAs) currently under evaluation as biomaterial has expanded to five, that is, poly[(*R*)-3-hydroxybutyrate] [P(3HB)], poly(4-hydroxybutyrate) [P(4HB)], poly[(*R*)-3-hydroxybutyrate-*co*-4-hydroxybutyrate] [P(3HB-*co*-4HB)], poly[(*R*)-3-hydroxybutyrate-*co*-(*R*)-3-hydroxyvalerate] [P(3HB-*co*-3HV)] and poly[(*R*)-3-hydroxyoctanoate-*co*-(*R*)-3-hydroxyhexanoate]

[P(3HO-*co*-3HHx)] [1]. To date, PHA and its composites are thought to have good potentials as emerging materials for medical devices such as sutures, bone plates, surgical mesh and cardiovascular patches, just to name a few [2]. A recent major breakthrough for PHA as a new class of biomaterial is the clearance obtained from the Food and Drug Administration of the United States of America for the use of P(4HB)-derived Tephaflex[®] absorbable suture [3].

PHAs are a family of biopolyesters produced by numerous bacteria as intracellular carbon and energy compound under unfavorable growth conditions such as limitation of nitrogen, phosphorus, oxygen or magnesium in the presence of excess supply of carbon source [4–6]. PHAs are particularly attractive because they are bioabsorbable and biocompatible. The metabolism and excretion of some monomers incorporated into PHA

* Corresponding author. Tel.: +81 48 467 9312; fax: +81 48 462 4658.

** Corresponding author. Tel.: +81 3 5841 7888; fax: +81 3 5841 1304.

E-mail addresses: mfujita@riken.jp (M. Fujita), atiwata@mail.ecc.u-tokyo.ac.jp (T. Iwata).

are well understood. For example, the monomeric component of P(3HB), (*R*)-3-hydroxybutanoic acid (3HB), is a ketone body present at concentrations of 3–10 mg per 100 mL blood in healthy adults [1,7]. The monomeric component of P(4HB), 4-hydroxybutanoic acid (4HB), can also be found widely distributed in the brain, kidney, heart, liver, lung and muscle of the mammalian body [8]. Furthermore, the hydroxyl acids released during PHA *in vivo* breakdown are found to be considerably less acidic and less inflammatory than many currently used synthetic absorbable polymers such as poly(lactic acid) (PLA) [9]. P(3HB) has, however, limited application due to its high brittleness, poor processability and slow degradation [10]. Therefore, researches in this field of interest had shown great progress over the past 20 years and it is now possible to design and synthesize various kinds of PHA (reviewed in Ref. [11]) to overcome the inferior properties of P(3HB).

New polymer processing approaches are in demand to create degradable porous scaffolds that can support the hierarchical structures of many tissues ranging between 0.1 and 1.0 mm [12]. Electrospinning has emerged as one of the methods offering simplicity and versatility in preparing such biomaterials [13]. Electrospun biomaterials facilitate better cell attachment and perfusion due to very high surface area-to-volume ratio and high porosity. Improved cellular response is also suggested because the morphology and architecture of electrospun structure are similar to those of some extracellular matrix (ECM) [14]. In addition, electrospinning may provide an alternative method to produce fibrous materials with improved mechanical properties compared to solid-walled equivalents [15].

Thus, in this study, we used electrospinning to develop scaffolds of fibrous PHA copolymers; P(3HB-co-5mol%-3HHx), P(3HB-co-7mol%-4HB) and P(3HB-co-97mol%-4HB) (Fig. 1), in aim of achieving enhanced biocompatibility, mechanical properties and bioabsorption. We also describe here the characterization and effects of sterilization on the physical properties of the electrospun PHA copolymers. Our study is the first to do a detailed comparison on the bioabsorption rate and the tissue response of electrospun PHA copolymers containing 3HB, 3HHx and 4HB monomers implanted subcutaneously in rat model.

2. Materials and methods

2.1. PHA synthesis

P(3HB-co-97mol%-4HB) was biosynthesized by *Delftia acidovorans* (formerly known as *Comamonas acidovorans*) using glucose and 1,4-butanediol as carbon sources, according to the method described in Ref. [16]. P(3HB-co-7mol%-4HB) was kindly provided by Dr. Toshihisa Tanaka of RIKEN Institute, Japan. The *in vitro* toxicity of P(3HB-co-4HB) derived from *D. acidovorans* has been determined recently [17]. P(3HB) and P(3HB-co-5mol%-3HHx) supplied by ICI Biopol and P&G, respectively, were purified before use. Briefly, the purification of the P(3HB) and P(3HB-co-5mol%-3HHx) was performed by dissolving the polymers in chloroform followed by precipitation in excess hexane and filtration.

2.2. Fabrication of fibrous implant and electrospinning

Each polymer solution of 1 wt% concentration was prepared by dissolving 100 mg of the polymer in 9900 mg of 1,1,1,3,3,3-hexafluoro-2-propanol

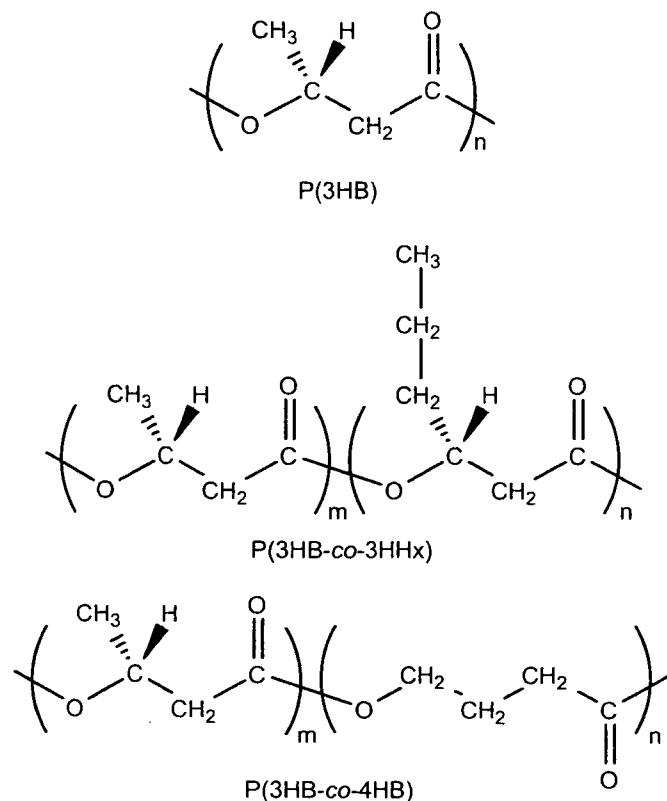


Fig. 1. Chemical structures of PHAs used in this study.

(HFIP). Electrospinning was performed using Esprayer ES-2000 (Fuence, Co. Ltd., Japan). The polymer solution was placed in a 1-mL glass syringe with an inner needle diameter of 0.5 mm. The syringe was set vertically at the support of the electrospinning device and the solution was extruded at a constant rate of 40 $\mu\text{L min}^{-1}$. A positive voltage of 15 kV was applied at a distance of 20 cm between the needle tip and the copper collecting plate. The jet current was in the range of 38.3–38.7 μA and the collecting time was approximately 8 h. For effective collection of the electrospun fibers, a square fiber-collecting area (3 cm \times 3 cm) was created on the copper plate by covering the rest of the plate with a non-conductive plastic. A sheet of aluminum foil was used to cover the collection area to ease the recovery of fibrous matrix from the copper plate. Each electrospun PHA scaffold was then cut into two different dimensions: 1 cm \times 1 cm and 1 cm \times 3 cm, respectively. All scaffolds were sterilized overnight with ethylene oxide (EtO) at 40 $^{\circ}\text{C}$ before implantation in rat.

2.3. Subcutaneous implantation in rat and retrieval

Four 12-week-old male Wistar rats were used for implanting the PHA scaffolds; two for scaffolds measuring 1 cm \times 1 cm while the remaining two for scaffolds measuring 1 cm \times 3 cm. The animals were cared for in accordance with the Guiding Principles for the Care and Use of Animals in the Field of Physiological Sciences, approved by the Physiological Society of Japan. All experiment protocols had been reviewed and approved by the Animal Subjects Committee of the National Cardiovascular Center, Osaka, Japan. The rats were first injected with anesthetic before implanting the scaffolds. The 1 cm \times 1 cm scaffolds were implanted subcutaneously at one side of the backbone while the 1 cm \times 3 cm scaffolds were implanted subcutaneously at the backbone. The grouping of the rats was based on the duration of observation for 4 and 12 weeks. Upon explantation, the scaffolds measuring 1 cm \times 1 cm were stored in 2.5% glutaraldehyde solution until further analysis by SEM. The retrieved 1 cm \times 3 cm scaffolds were treated with 1.25 wt% trypsin to remove the surrounding tissues. They were then kept in tubes containing phosphate buffered saline (PBS) until further use.

2.4. Scanning electron microscopy

The PHA scaffolds were dehydrated in increasing concentrations of ethanol aqueous solutions containing 50%, 70%, 90%, 95%, 99.5% and 100%. They were then mounted on aluminum stumps and coated with gold in a sputtering device for 3 min at 5 mA. The scaffolds were observed with a scanning electron microscope (JSM-6330F, JEOL, Co. Ltd.) at an acceleration voltage of 5 kV and an emission current of 12 μ A.

2.5. Wide-angle X-ray diffraction (WAXD)

Two-dimensional (2D) WAXD patterns of the electrospun PHA scaffolds were acquired using an X-ray diffractometer (RINT UltraX 18, Rigaku Japan) equipped with an imaging plate (BAS-SR 127, Fuji Film Co., Japan). Ni-filtered Cu-K α radiation ($\lambda = 0.154$ nm) generated at 40 kV and 200 mA was collimated by a pinhole with a diameter of 1.0 mm. The distance from the scaffold to the imaging plate was 5 cm and the exposure time was 6 h. After converting the 2D images to 1D profile by circular-averaging, the crystallinity of the scaffolds was calculated from the ratio of the areas of crystalline reflections to the overall intensity in the range of $12^\circ \leq 2\theta \leq 35^\circ$ of the averaged 1D profile.

2.6. Tensile property

The non-sterilized scaffolds and the scaffolds before and after implantation were cut into 2 mm \times 5 mm strips for tensile test. Tensile test on the scaffolds was carried out on a tensile testing machine (SHIMADZU EZTest) at a cross-head speed of 1 mm/min under ambient conditions. The thickness of each scaffold was measured before testing. Tensile properties were calculated from the stress–strain curves as means of two measurements.

2.7. Gel permeation chromatography (GPC) analysis

The molecular weight of the scaffolds was measured with gel permeation chromatography at 40 $^\circ$ C, using a Shimadzu 10A GPC system equipped with a 10A refractive index detector and Shodex K-806M and K-802 columns. Chloroform was used as the eluant at a flow rate of 1.0 ml min $^{-1}$. The calibration curve was prepared by using polystyrene standards with narrow polydispersity.

2.8. In vitro degradation evaluation

Each of the 1 cm \times 3 cm sterilized scaffold was immersed in 10 mL phosphate buffered saline (PBS) at pH 7.4 in sterilized capped containers. These containers were then incubated at 37 $^\circ$ C without agitation. After 4 and 12 weeks, the scaffolds were recovered and characterized by SEM, tensile test, GPC and WAXD.

2.9. Histological observation

The surrounding tissues were excised together with the electrospun PHA scaffolds and fixed with 2.5% glutaraldehyde solution. A small piece of the tissue was then embedded in paraffin before subjecting it to microtome sectioning. Hematoxylin and eosin (HE) were used for staining the tissues. The tissue response to the scaffolds was evaluated from the coloration observed with a phase-contrast microscope.

3. Results and discussion

3.1. Morphological changes of electrospun PHA scaffolds

The retrieved electrospun PHA scaffolds showed various changes in appearances after subcutaneous implantation

(Fig. 2). After 4 weeks, both the electrospun P(3HB) and P(3HB-co-5mol%-3HHx) remained in their initial form. The electrospun P(3HB-co-7mol%-4HB) was fragmented into large pieces while the electrospun P(3HB-co-97mol%-4HB) shrunk and became thinner. Even after 12 weeks, the electrospun P(3HB) showed no morphological change. However, significant changes were observed for the other three electrospun PHA copolymers. The degree of degradation increased in the order of P(3HB-co-5mol%-3HHx), P(3HB-co-7mol%-4HB), and (3HB-co-97mol%-4HB). The electrospun P(3HB-co-5mol%-3HHx) displayed crevices on its surface while the electrospun P(3HB-co-7mol%-4HB) was degraded into small fragments. Only a small piece of the electrospun P(3HB-co-97mol%-4HB) scaffold was retrieved, indicating enhanced bioabsorption of this 4HB-rich copolymer.

To have a better understanding on the progress of biodegradation at a fiber scale, SEM was used to observe the morphological changes of the fibers of all the electrospun PHA scaffolds. SEM revealed that all the as-spun scaffolds consist of randomly oriented fibers (Figs. 3 and 4). Further morphological feature is that the fibers fuse together. Namely, the electrospun fibers organize into a three-dimensional network. This is probably because the solvent (HFIP) evaporation was incomplete when the fibers were deposited on the collection plate. The width of the fiber between the junctions was quite uniform. The width decreased in the order of P(3HB) \approx P(3HB-co-5mol%-3HHx) (520 nm) > P(3HB-co-97mol%-4HB) (220 nm) > P(3HB-co-7mol%-4HB) (190 nm). It has been reported that the width increases proportionally with the molecular weight of the polymer [18]. This is because higher degree of chain entanglement due to high molecular weight is assumed to make it harder for the electrostatic forces to pull, or extend individual chains [19]. Accordingly, the matrices of the electrospun P(3HB) and P(3HB-co-5mol%-3HHx) consisted of larger fibers compared to the electrospun P(3HB-co-97mol%-4HB) because of their high molecular weight (Table 1).

Interestingly, only the electrospun P(3HB-co-7mol%-4HB) formed fibers with irregular shapes with intermittent spindle-like beads on string (Fig. 4A). Possibly the formation of the beaded P(3HB-co-7mol%-4HB) fibers is the result of low net charge density. Previous studies have shown that higher net charge density favors the formation of bead-free fibers [20,21]. According to Ref. [20], the net charge density is inversely proportional to the mass of dry polymer (i.e. mass of scaffolds collected from electrospinning), if the other experimental conditions such as jet current, collecting time and polymer concentration are the same. The net charge density decreases in the order of P(3HB-co-5mol%-3HHx) (1058 C/l) > P(3HB) (1002 C/l) > P(3HB-co-97mol%-4HB) (778 C/l) > P(3HB-co-7mol%-4HB) (484 C/l). In this study, the P(3HB-co-7mol%-4HB) scaffold had the highest collected mass.

After sterilization, the morphologies observed for the electrospun P(3HB), P(3HB-co-5mol%-3HHx) and P(3HB-co-7mol%-4HB) remained unchanged (Figs. 3 and 4). The matrix of P(3HB-co-97mol%-4HB), however, became less porous

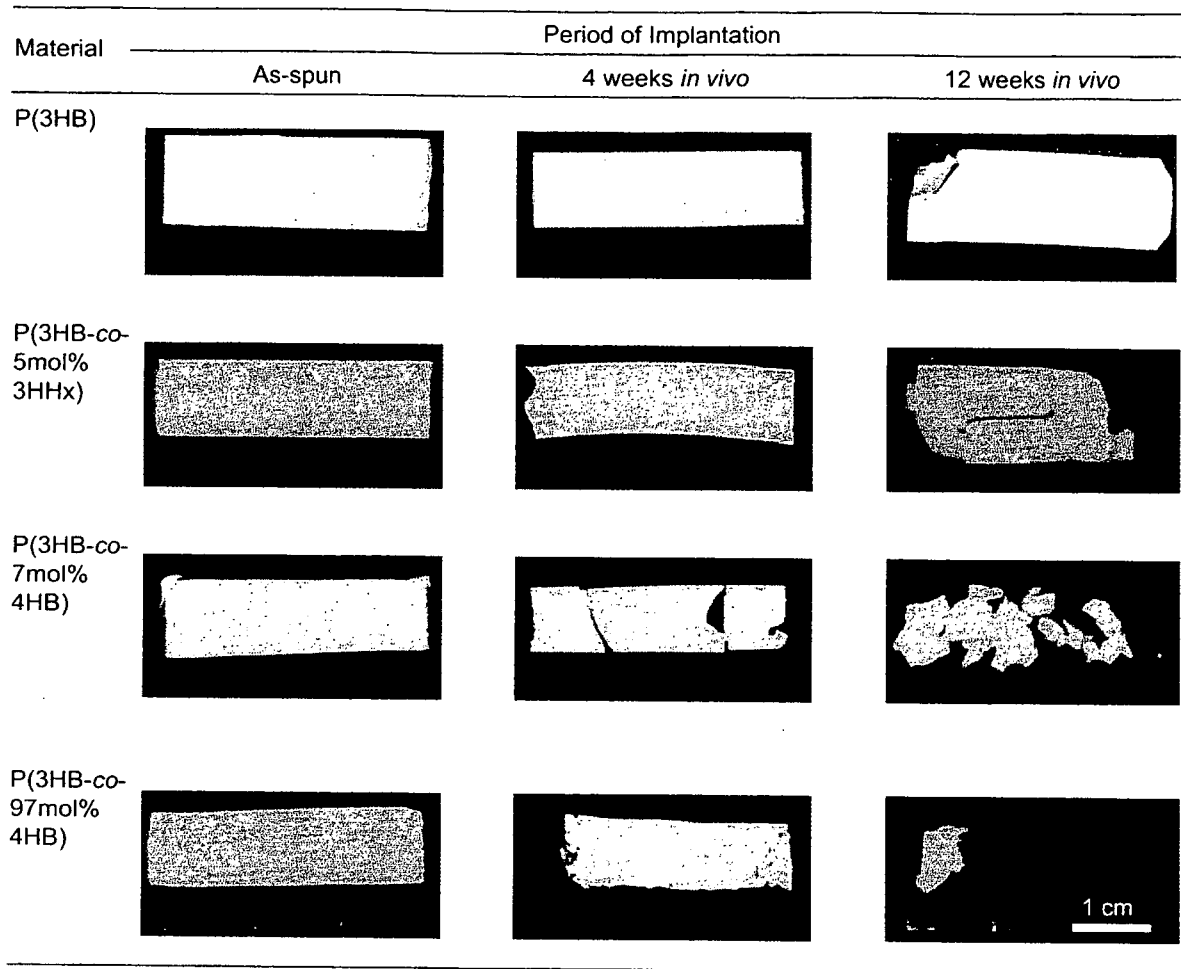


Fig. 2. Physical appearance of the electrospun PHA scaffolds before and after 4 and 12 weeks of subcutaneous implantation in rat.

(Fig. 4B2). The temperature (40 °C) of the EtO sterilization is close to the melting temperature of P(3HB-co-97mol%-4HB) ($T_m = 47$ °C), and thus led to the fusing of some fibers to each other.

3.1.1. *In vivo* study

In SEM, only the remaining scaffolds that could be retrieved from rat after the *in vivo* experiments were observed. Nevertheless, such observations provided the information on the morphological changes by implantation. For the P(3HB) and P(3HB-co-5mol%-3HHx) scaffolds, no remarkable change in their appearances by implantation during the period investigated here was observed (Fig. 3). This result is in good agreement with the macro-scale observation, as shown in Fig. 2. On the other hand, the fibers of the copolymers with 4HB unit were influenced by the implantation. At 4 weeks of implantation, the fibers of P(3HB-co-97mol%-4HB) showed fragmentation (Fig. 4B3). After 12 weeks, surface erosion became more evident as the density of the fibers decreased remarkably due to fragmentation of the fibers to shorter segments. The progression of bioabsorption was also evidenced by the formation of pores on the surface of these fibers as indicated by the arrow in Fig. 4B4. These evidences

indicate that the existence of 4HB monomer units enhances the degradability, or the bioabsorption of PHA.

After 4 and 12 weeks, the electrospun P(3HB-co-97mol%-4HB) fibers appeared to have swollen (Fig. 4B3 and B4). A slight decrease in the fiber density was also observed for the electrospun P(3HB-co-7mol%-4HB) (Fig. 4A4) at week 12. Previous studies have demonstrated that fibers of electrospun poly(D,L-lactic-co-glycolic acid), poly(D,L-lactic acid) and poly(butylene succinate) which were highly amorphous showed swelling after immersion in PBS [22–24]. Hence, it is possible that the swelling of the electrospun P(3HB-co-97mol%-4HB) fibers occurred due to the penetration of water into their amorphous regions.

3.1.2. *In vitro* study

SEM showed that there was no evidence of degradation on the surface of all the electrospun PHA scaffolds after 4 weeks of immersion in PBS (Figs. 3 and 4). All samples retrieved at 12 weeks also revealed that their structural integrities were maintained. This is because PHA hardly undergoes hydrolysis at pH value around neutrality. Similar to the observations for the *in vivo* study, the fibers of the electrospun P(3HB-co-97mol%-4HB) also demonstrated swelling.


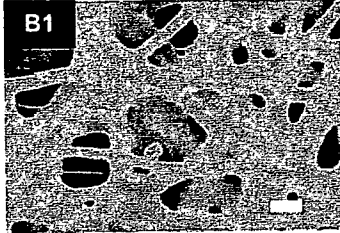
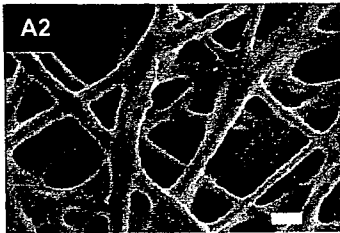

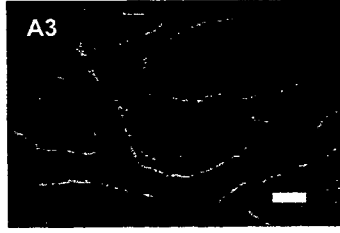

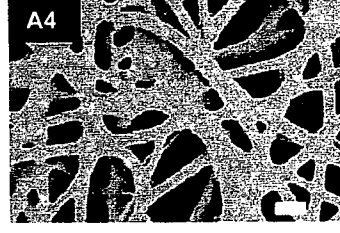


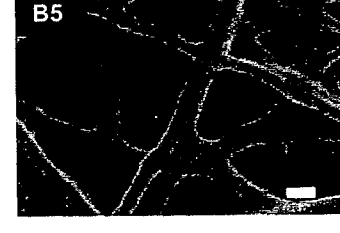
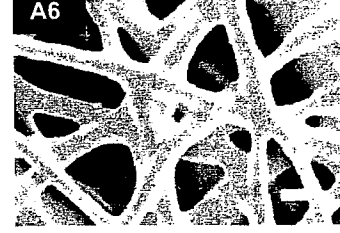
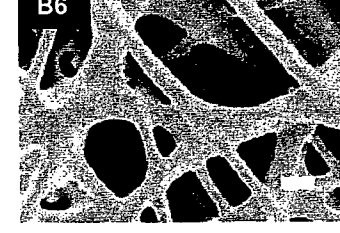
Condition	Material	
	P(3HB)	P(3HB-co-5mol%-3HHx)
As-spun		
Sterilized		
4 weeks <i>in vivo</i>		
12 weeks <i>in vivo</i>		
4 weeks <i>in vitro</i>		
12 weeks <i>in vitro</i>		

Fig. 3. SEM micrographs of the electrospun P(3HB) and P(3HB-co-5 mol%-3HHx) in various conditions.

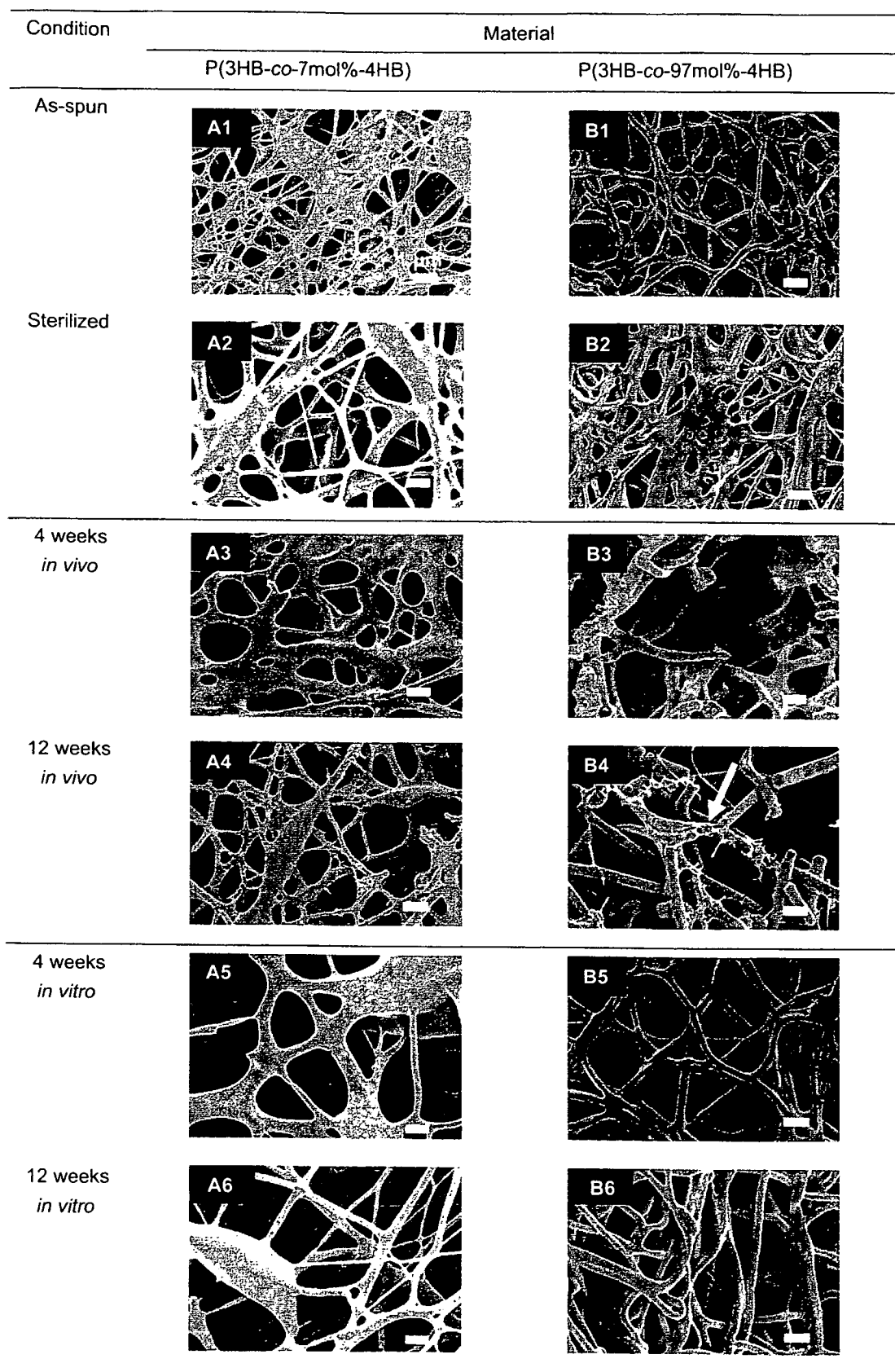


Fig. 4. SEM micrographs of the electrospun P(3HB-co-7 mol%-4HB) and P(3HB-co-97 mol%-4HB) in various conditions. The arrow shows the pores on the fiber.

Table 1
Molecular weight properties of the electrospun PHA scaffolds

Material	Condition	$M_w \times 10^5$	M_w/M_n
P(3HB)	As-spun	11	3.1
	Sterilized	9.1	3.3
	4 weeks <i>in vivo</i>	12	2.6
	4 weeks <i>in vitro</i>	11	2.6
	12 weeks <i>in vivo</i>	8.5	2.9
	12 weeks <i>in vitro</i>	17	3.3
P(3HB-co-5mol%-3HHx)	As-spun	13	3.6
	Sterilized	12	3.6
	4 weeks <i>in vivo</i>	12	3.1
	4 weeks <i>in vitro</i>	11	4.3
	12 weeks <i>in vivo</i>	11	3.3
	12 weeks <i>in vitro</i>	13	4.3
P(3HB-co-7mol%-4HB)	As-spun	7.0	3.0
	Sterilized	6.8	3.0
	4 weeks <i>in vivo</i>	6.4	2.6
	4 weeks <i>in vitro</i>	6.1	2.6
	12 weeks <i>in vivo</i>	3.9	2.7
	12 weeks <i>in vitro</i>	5.0	2.6
P(3HB-co-97mol%-4HB)	As-spun	1.7	1.5
	Sterilized	1.9	1.8
	4 weeks <i>in vivo</i>	1.0	1.6
	4 weeks <i>in vitro</i>	2.5	2.0
	12 weeks <i>in vivo</i>	1.2	2.0
	12 weeks <i>in vitro</i>	2.2	1.8

The *in vivo* and *in vitro* observations using SEM revealed that fibers with smaller diameter were more prone to fragmentation because of increased water contact due to large surface area. Thus, it can be concluded that surface erosion of the electrospun PHA scaffolds depends upon individual fiber dimensions and monomeric content.

3.2. Crystallinity

The WAXD profiles of the as-spun PHA scaffolds are displayed in Fig. 5. The profiles are the ones after subtraction of background. As shown in this figure, the crystalline reflections for the P(3HB) and the 3HB-rich copolymers could be indexed on the basis of P(3HB) α -form structure [25] while the crystalline phase of P(3HB-co-97mol%-4HB) fibers adopted the P(4HB) crystal structure [26]. From the 1D profiles, the crystallinity of as-spun, sterilized and scaffolds after *in vivo* and *in vitro* studies is estimated, according to the method described above. As shown in Fig. 6, the crystallinity of the as-spun PHA scaffolds increased in the order of P(3HB-co-97mol%-4HB) < P(3HB-co-5mol%-3HHx) \approx P(3HB-co-7mol%-4HB) < P(3HB). This tendency is the same as the case of those bulk materials [27]. It has been reported that the crystallinity of P(4HB) homopolymer is much lower than that of P(3HB) homopolymer [28]. The slight lowering of the crystallinities of the 3HB-rich copolymers is due to the exclusion of second monomer unit from the crystalline lattice [29]. It is evident that the degradability of the scaffolds, as shown in Figs. 2 and 3, strongly depends on the crystallinity.

We confirmed that the EtO sterilization did not appear to have any effect on the crystallinities of all the electrospun

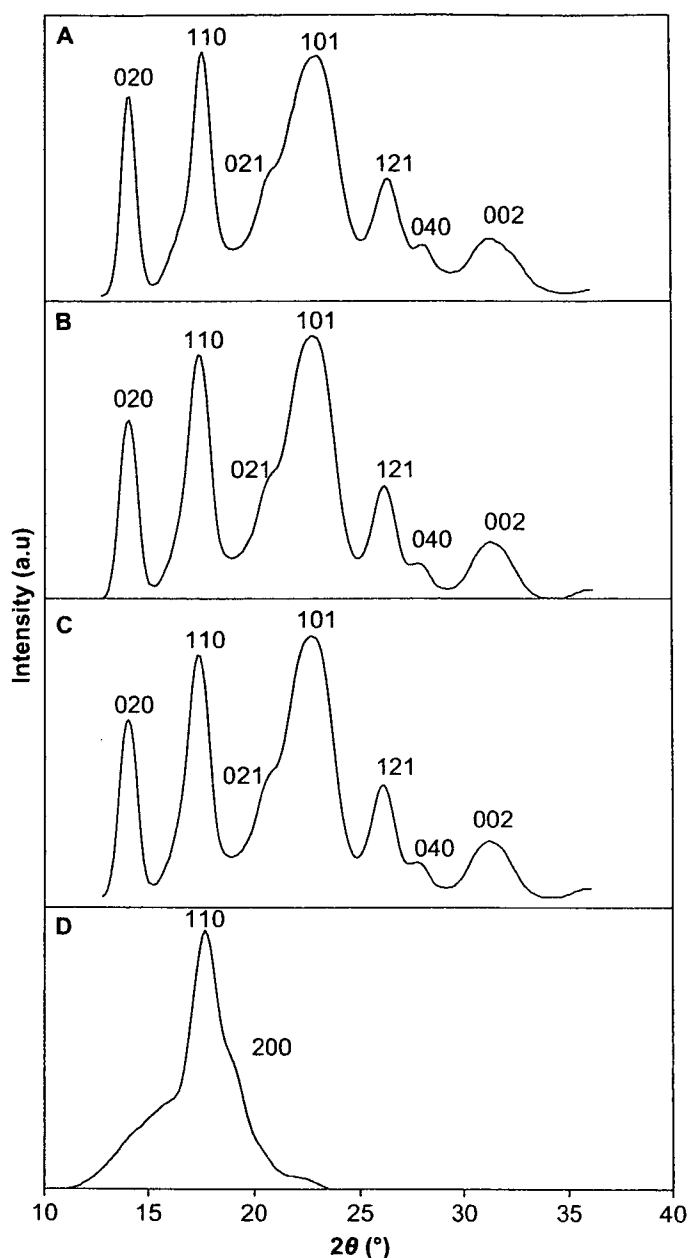


Fig. 5. Integrated 1D profiles from 2D WAXD patterns of as-spun: (A) P(3HB), (B) P(3HB-co-5 mol%-3HHx), (C) P(3HB-co-7 mol%-4HB) and (D) P(3HB-co-97 mol%-4HB).

PHA scaffolds. We described earlier that partial melting might occur during the sterilization of P(3HB-co-97mol%-4HB). Even if so, the crystallinity will surely recover after the sterilization. The crystallinities of the scaffolds after the *in vivo* and *in vitro* studies remained unchanged. But, it should be noted that the scaffolds for X-ray measurements are the retrieved or remained ones after *in vivo* and *in vitro* experiments. The crystallinity of the P(3HB-co-97mol%-4HB), which shows obvious bioabsorption or degradation in the macro-scale and SEM observations, also little changed even after implantation in rat. This means that the degradation of scaffolds progresses preferentially from the surface of the scaffolds or interface which contacts with the tissues of rat. It is deduced that some substance such as tissue enzymes facilitate the degradation [30].

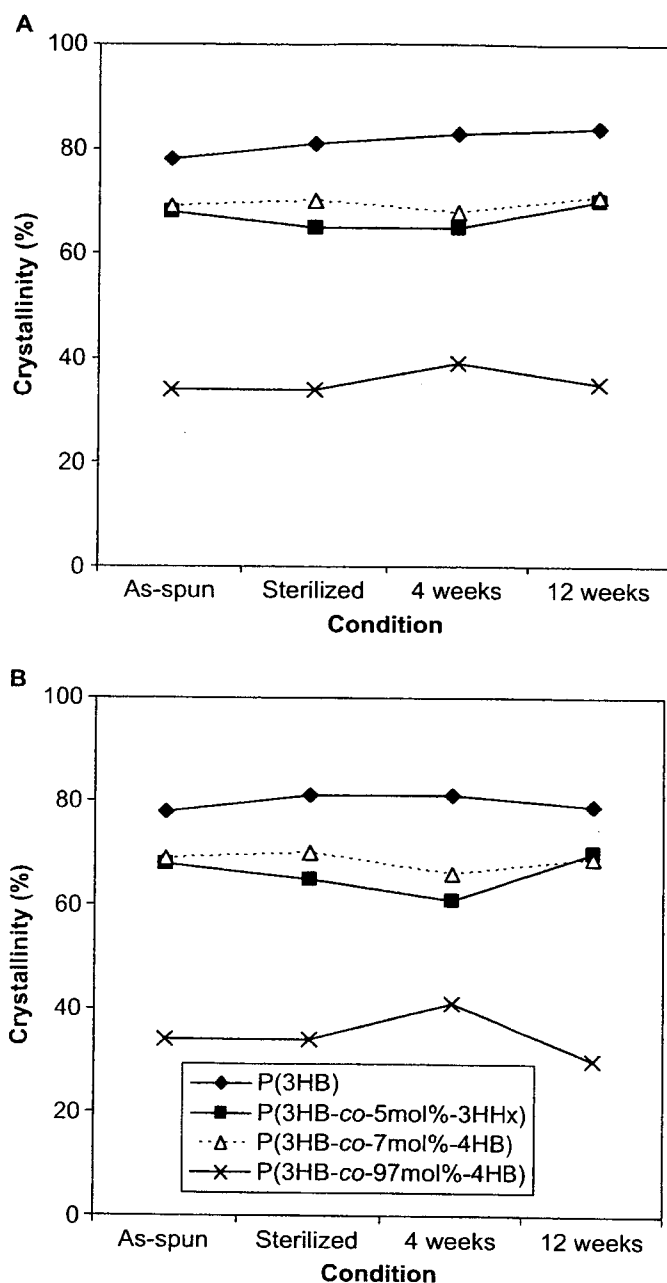


Fig. 6. Crystallinities of the electrospun PHA scaffolds in different conditions: (A) *in vivo* and (B) *in vitro*.

3.3. Molecular weight changes of electrospun PHA scaffolds

Table 1 summarizes the change in M_w and polydispersity index (M_w/M_n) for the as-spun scaffolds and scaffolds following sterilization, 4 and 12 weeks of *in vivo* and *in vitro* studies. After sterilization, all of the electrospun PHA scaffolds showed no significant differences in their molecular weight. Despite the large surface area of the fibers, PHA scaffolds remained intact in the *in vitro* study because they have higher resistance to hydrolysis in non-biological environment where specific enzymes are absent [27,31]. Furthermore, the immersion in PBS (pH 7.4) under sterile conditions up to only 12 weeks is short and

the temperature is low for any significant hydrolysis to occur. The subcutaneous implantation, however, seems to cause decrease in the M_w of PHA copolymers with 4HB unit. At 4 weeks, bioabsorption was the most pronounced for the electrospun P(3HB-co-97mol%-4HB) with 47% loss M_w , while the M_w of P(3HB-co-7mol%-4HB) showed no decrease. Following longer implantation period, the electrospun P(3HB-co-7mol%-4HB) lost 43% of M_w . Unexpectedly, the electrospun P(3HB-co-97mol%-4HB) recorded only 37% of M_w loss after 12 weeks. It was confirmed that the number of main-chain carbon atom strongly influences the rate of hydrolysis.

3.4. Mechanical properties of electrospun PHA scaffolds

Table 2 summarizes the mechanical properties of electrospun PHA scaffolds obtained. The mechanical properties of all the as-spun scaffolds were comparable to those of human skin, and hence suggest they are mechanically stable in supporting regenerated tissues. The Young's modulus of the as-spun scaffolds increased in the order of P(3HB-co-97mol%-4HB) \ll P(3HB-co-7mol%-4HB) $<$ P(3HB) $<$ P(3HB-co-5mol%-3HHx). Low Young's modulus, that is, high elasticity is a characteristic property in rubber-state amorphous polymers. Accordingly, this

Table 2
Mechanical properties of the PHA scaffolds

Material	Condition	Mechanical properties	
		Tensile strength (MPa)	Young's modulus (MPa)
P(3HB)	As-spun	17	223
	Sterilized	15	234
	4 weeks <i>in vivo</i>	12	182
	4 weeks <i>in vitro</i>	14	220
	12 weeks <i>in vivo</i>	15	152
	12 weeks <i>in vitro</i>	13	194
P(3HB-co-5mol%-3HHx)	As-spun	15	277
	Sterilized	12	272
	4 weeks <i>in vivo</i>	12	268
	4 weeks <i>in vitro</i>	13	208
	12 weeks <i>in vivo</i>	ND ^b	ND ^b
	12 weeks <i>in vitro</i>	15	230
P(3HB-co-7mol%-4HB)	As-spun	8	184
	Sterilized	8	139
	4 weeks <i>in vivo</i>	ND ^b	ND ^b
	4 weeks <i>in vitro</i>	8	163
	12 weeks <i>in vivo</i>	ND ^b	ND ^b
	12 weeks <i>in vitro</i>	9	110
P(3HB-co-97mol%-4HB)	As-spun	13	9
	Sterilized	15	16
	4 weeks <i>in vivo</i>	4	12
	4 weeks <i>in vitro</i>	11	14
	12 weeks <i>in vivo</i>	ND ^b	ND ^b
	12 weeks <i>in vitro</i>	14	16
Skin ^a		5–30	15–150

^a Data obtained from Ref. [13].

^b Not determined as the retrieved scaffolds from rat had cracks on the surface that prevented tensile test.

indicates that the P(3HB-co-97mol%-4HB) fibers are more amorphous than the other scaffolds, and this is consistent with the WAXD results. The distinct mechanical properties of the PHA could find different use as scaffolds for tissue engineering. For example, the 3HB-rich scaffolds which are more rigid could serve as preferential substrates for directional cell migration [32] while the compliant 4HB-rich scaffolds could be used to promote cell motility [33]. The EtO sterilization and the immersion in PBS buffer little affected the mechanical properties of all the scaffolds.

3.5. Histological observation

The histological sections of the electrospun PHA scaffolds at different period of subcutaneous implantation are shown in Fig. 7. Histological observations indicate that all the three electrospun copolymers elicited fairly mild tissue response relative to that of the electrospun P(3HB) throughout the course of study. After 4 weeks of implantation, some parts of the electrospun P(3HB-co-97mol%-4HB) bordering the interface were degraded as evidenced by the small fragments broken off from

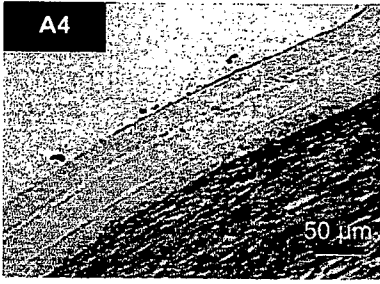
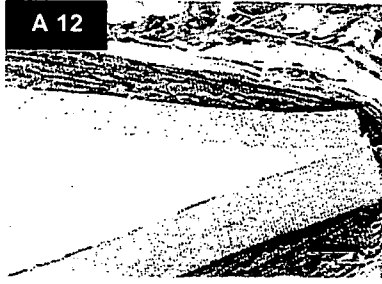
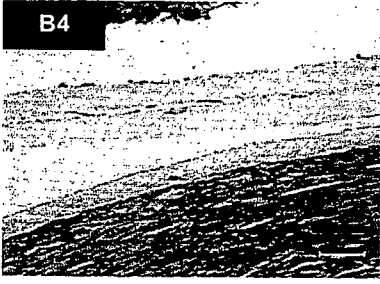
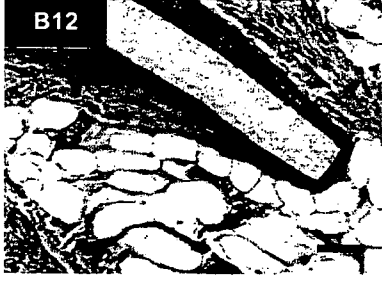
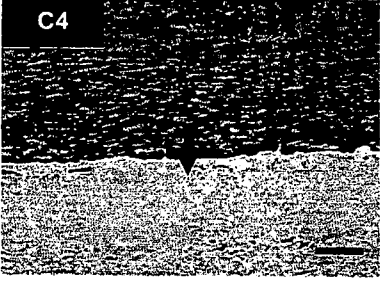
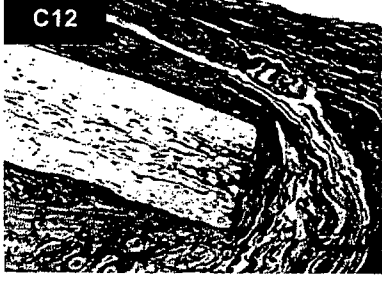
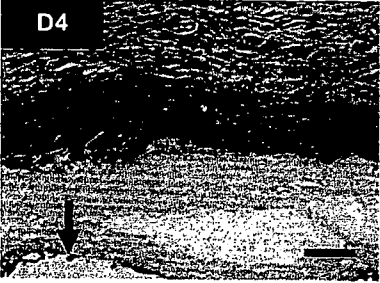
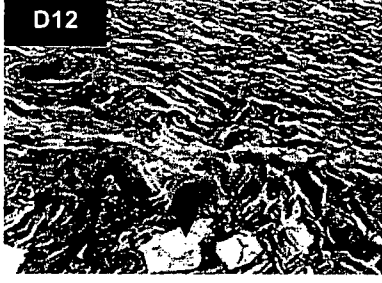
Material	Period of Implantation	
	4 weeks	12 weeks
P(3HB)		
P(3HB-co-5mol%-3HHx)		
P(3HB-co-7mol%-4HB)		
P(3HB-co-97mol%-4HB)		

Fig. 7. Histological sections of the electrospun PHA scaffolds at different period of subcutaneous implantation. Arrows indicate the polymer surface.

the main scaffold (Fig. 7D4). More macrophages were found to be present along the interface connected to this copolymer in comparison to the electrospun P(3HB-co-7mol%-4HB) and P(3HB-co-5mol%-3HHx) (Fig. 7B4 and C4). This phenomenon is desirable during wound healing because the presence of macrophages is necessary for the regeneration of many cell types [34]. The presence of thin connective tissue surrounding the electrospun P(3HB-co-97mol%-4HB) was also observed.

The most promising finding was the tissue response after 12 weeks of implantation for the electrospun P(3HB-co-97mol%-4HB). No fibrous encapsulation was observed around the degraded copolymer and there was also a substantial drop in the number of inflammatory cells (Fig. 7D12). This observation is similar to a study done on the biocompatibility of P(4HB) implanted subcutaneously in rats by Martin et al. [35], that reported minimal inflammatory responses. In this study, the number of inflammatory cells surrounding the electrospun P(3HB-co-7mol%-4HB) and P(3HB-co-5mol%-3HHx) did not appear to have lessened. The muscle cells surrounding these two scaffolds appeared compact as a result of inflammatory reaction (Fig. 7B and C). After 12 weeks of implantation, the number of macrophages bordering the electrospun P(3HB) increased. Inflammation was obvious due to the compacted muscle cells surrounding the scaffold. The difference in tissue response to the electrospun P(3HB-co-97mol%-4HB) and the electrospun scaffolds with higher molar fraction of 3HB reflected their distinct physical properties. It has been reported that rigid polymer, such as P(3HB), elicit acute inflammatory reaction because it exerts a continuous mechanical stimulus to the surrounding tissues of the implants [36]. Although the tissue response to the electrospun P(3HB-co-7mol%-4HB) and electrospun P(3HB-co-5mol%-3HHx) was slightly more pronounced than that of the electrospun P(3HB-co-97mol%-4HB), the overall local tissue response to all three copolymers was found to be mild. The results have confirmed the biocompatibility of all three types of electrospun PHA copolymers.

3.6. Bioabsorption mechanism

The results from various analyses clearly demonstrated that the bioabsorption rate of the electrospun P(3HB-co-97mol%-4HB) was the fastest relative to the other two PHA copolymers. Three possible reasons for this observation are as follows: Firstly, the P(3HB-co-97mol%-4HB) with low crystallinity is more susceptible to bioabsorption as water and enzymes penetrate easier into the amorphous regions. Secondly, previous studies have established that macrophages are able to phagocytize PHA *in vitro* [37,38] and free radicals, acidic products or enzymes produced by these cells may also accelerate the degradation [39]. As seen in Fig. 7, the number of inflammatory cells was the most concentrated at the interface of electrospun P(3HB-co-97mol%-4HB) suggesting their active part in the bioabsorption process. Thirdly, possibly the enzymatic degradation by lipase also contributed to the rapid bioabsorption of the electrospun P(3HB-co-97mol%-4HB). PHA can be enzymatically degraded by PHA depolymerases, but there is no

evidence to date that these are present *in vivo* [1]. P(4HB) was found to be also highly susceptible to lipase hydrolysis as opposed to P(3HB) [40]. Besides having good mechanical properties and biocompatibility, it is desirable for a medical implant to show good bioabsorption after its primary function has been fulfilled. The persistence of polymer at a wound healing site may lead to chronic inflammation as shown by the slowly degrading P(3HB) patches that elicited a long-term (greater than 2 years) macrophage response [41]. Hence the fast bioabsorption rates of the electrospun PHA containing 4HB have confirmed their potential in the application for medical implants.

4. Conclusion

In this study, electrospinning proved to be a simple and adaptable fabrication technique in producing constructs with dimensions approaching the native profile of ECM. Sterilization did not cause discoloration and damage to the PHA scaffolds. SEM revealed that both the *in vivo* and *in vitro* surface erosion of the electrospun PHA scaffolds progressed dependently on the individual fiber dimensions and monomeric contents. The mechanical properties demonstrated by all samples were comparable to those of human skin thus suggesting that their structures are able to provide sufficient biomechanical support. The electrospun scaffolds consisting of high 3HB content had higher degree of crystallinity and thus, they showed slower bioabsorption rate. GPC revealed that the *in vitro* degradation of the electrospun PHA scaffolds proceeded at a much slower rate in comparison to the *in vivo* bioabsorption. Histological evaluation showed that subcutaneous implantations of the electrospun PHA scaffolds were well tolerated *in vivo* as the tissue response continued to be very mild throughout the course of the study. Our results revealed that by changing the molar fraction of monomers in the PHA copolymers, it is possible to create tissue-engineering scaffolds that are tailor-made to meet the various needs in regenerating different cell type. The electrospun PHA copolymers proved to be promising biomaterials for scaffolds because of their biodegradability, flexible mechanical properties and excellent biocompatibility.

Acknowledgement

This work was supported by a Grant-in Aid for Scientific Research (B) from the Ministry of Education, Culture, Sports, Science and Technology (MEXT) of Japan (No.19350075) (to T. Iwata) and by a grant for Ecomolecular Science Research II provided by RIKEN Institute.

References

- [1] Williams SF, Martin DP. Applications of PHAs in medicine and pharmacy. In: Steinbüchel A, editor. Series of biopolymers in 10 volumes, vol. 4. Wiley/VCH/Verlag; 2002. p. 91–121.
- [2] Chen GQ, Wu Q. The application of polyhydroxyalkanoates as tissue engineering materials. *Biomaterials* 2005;26:6565–78.
- [3] FDA clears first of its kind suture made using DNA technology. Available from: FDA News <http://www.fda.gov/bbs/topics/NEWS/2007/NEW01560.html>; 2007 February 12 [accessed 25.04.07].

- [4] Anderson AJ, Dawes EA. Occurrence, metabolic role, and industrial uses of bacterial polyhydroxyalkanoates. *Microbiol Rev* 1990;54:450–72.
- [5] Doi Y. *Microbial polyesters*. New York: VCH; 1990.
- [6] Kato M, Bao HJ, Kang CK, Fukui T, Doi Y. Production of a novel copolyester of 3-hydroxybutyric acid and medium-chain-length 3-hydroxyalkanoic acids by *Pseudomonas* sp. 61-3 from sugars. *Appl Microbiol Biotechnol* 1996;45:363–70.
- [7] Hocking PJ, Marchessault RH. Biopolyesters. In: Griffin GJL, editor. *Chemistry and technology of biodegradable polymers*. London: Chapman & Hall; 1994. p. 48–96.
- [8] Nelson T, Kaufman E, Kline E, Sokoloff L. The extraneural distribution of gamma-hydroxybutyrate. *J Neurochem* 1981;37:1345–88.
- [9] Taylor MS, Daniels AU, Andriano KP, Heller J. Six absorbable polymers: *in vitro* acute toxicity of accumulated degradation products. *J Appl Biomater* 1994;5:151–7.
- [10] Iwata T, Tsunoda K, Aoyagi Y, Kusaka S, Yonezawa N, Doi Y. Mechanical properties of uniaxially cold-drawn films of poly[(R)-3-hydroxybutyrate]. *Polym Degrad Stab* 2003;217–24.
- [11] Sudesh K, Abe H, Doi Y. Synthesis, structure and properties of polyhydroxyalkanoates: biological polyesters. *Prog Polym Sci* 2000;25:1503–55.
- [12] Griffith LG. Emerging design principles in biomaterials and scaffolds for tissue engineering. *Ann N Y Acad Sci* 2000;961:83–95.
- [13] Zong X, Bien H, Chung CY, Yin L, Fang D, Hsiao BS, et al. Electrospun fine-textured scaffolds for heart tissue constructs. *Biomaterials* 2005;26:5330–8.
- [14] Li WJ, Laurencin CT, Cateson EJ, Tuan RS, Ko FK. Electrospun nanofibrous structure: a novel scaffold for tissue engineering. *J Biomed Res* 2002;60:613–21.
- [15] Kim J, Reneker DH. Mechanical properties of composites using ultrafine electrospun fibers. *Polym Composites* 1999;20:124–31.
- [16] Lee WH, Azizan MNM, Sudesh K. Effects of culture conditions on the composition of poly(3-hydroxybutyrate-co-4-hydroxybutyrate) synthesized by *Comamonas acidovorans*. *Polym Degrad Stab* 2004;84:129–34.
- [17] Siew EL, Rajab NF, Osman A, Sudesh K, Inayat-Hussain SH. *In vitro* biocompatibility evaluation of poly(3-hydroxybutyrate-co-4-hydroxybutyrate) copolymer in fibroblast cells. *J Biomed Res A* 2007;81A:317–25.
- [18] Dong H, Nyame V, Macdiarmid Jr AG, Jones WE. Polyaniline/poly(methyl methacrylate) coaxial fibers: the fabrication and effects of the solution properties on the morphology of electrospun core fibers. *J Polym Sci Part B: Polym Phys* 2004;42:3934–42.
- [19] Lyons J, Li C, Ko F. Melt-electrospinning part I: processing parameters and geometric properties. *Polymer* 2004;45:7597–603.
- [20] Fong H, Chun I, Reneker DH. Beaded nanofibers formed during electrospinning. *Polymer* 1999;40:4585–92.
- [21] Zuo W, Zhu M, Yang W, Yu H, Chen Y, Zhang Y. Experimental study on relationship between jet stability and formation of beaded fibers during electrospinning. *Polym Eng Sci* 2005;45:704–9.
- [22] Zong X, Ran S, Kim KS, Fang D, Hsiao BS, Chu B. Structure and morphology changes during *in vitro* degradation of electrospun poly(glycolide-co-lactide) nanofiber membrane. *Biomacromolecules* 2003;4:416–23.
- [23] Li WJ, Cooper Jr JA, Mauck RL, Tuan RS. Fabrication and characterization of six electrospun poly(α -hydroxyester)-based fibrous scaffolds for tissue engineering applications. *Acta Biomaterialia* 2006;2:377–85.
- [24] Jeong EH, Im SS, Youk JH. Electrospinning and structural characterization of ultrafine poly(butylene succinate) fibers. *Polymer* 2005;46:9538–43.
- [25] Yokouchi M, Chatani Y, Tadokoro H, Teranishi K, Tani H. Structural studies of polyesters: 5. Molecular and crystal structures of optically active and racemic poly(β -hydroxybutyrate). *Polymer* 1973;14:267–72.
- [26] Su F, Iwata T, Tanaka F, Doi Y. Crystal structure and enzymatic degradation of poly(4-hydroxybutyrate). *Macromolecules* 2003;36:6401–9.
- [27] Doi Y, Kanesawa Y, Kawaguchi Y, Kunioka M. Biodegradation of microbial polyesters in the marine environment. *Polym Degrad Stab* 1992;32:173–7.
- [28] Mitomo H, Hsieh WC, Nishiwaki K, Kasuya K, Doi Y. Poly(3-hydroxybutyrate-co-4-hydroxybutyrate) produced by *Comamonas acidovorans*. *Polymer* 2001;42:3455–61.
- [29] Di Lorenzo ML, Raimo M, Cascone E, Martuscelli E. Poly(3-hydroxybutyrate)-based copolymers and blends: influence of a second component on crystallization and thermal behavior. *J Macromol Sci Phys* 2001;40:639–67.
- [30] Gogolewski S. Resorbable polymers for internal fixation. *Clin Mater* 1992;10:13–20.
- [31] Marois Y, Zhang Z, Vert M, Deng X, Lenz R, Guidoin R. Mechanism and rate of degradation of polyhydroxyoctanoate films in aqueous media: a long term *in vitro* study. *J Biomed Mater Res* 2000;49:216–24.
- [32] Lo CM, Wang HB, Dembo M, Wang YL. Cell movement is guided by the rigidity of the substrate. *Biophys J* 2000;79:144–52.
- [33] Pelham RJ, Wang YL. Cell locomotion and focal adhesions are regulated by substrate flexibility. *Proc Natl Acad Sci U S A* 1997;94:13661–5.
- [34] Rappolee DA, Mark D, Banda MJ, Werb Z. Wound macrophages express TGF- α and other growth factors *in vivo*: analysis by mRNA phenotyping. *Science* 1988;241:708.
- [35] Martin DP, Skraly FA, Williams SF. Polyhydroxyalkanoate compositions having controlled degradation rates. PCT Patent Application No. WO 99/32536; 1999.
- [36] Qu XH, Wu Q, Zhang KY, Chen GQ. *In vivo* studies of poly(3-hydroxybutyrate-co-3-hydroxyhexanoate) based polymers: biodegradation and tissue reactions. *Biomaterials* 2006;27:3540–8.
- [37] Ali SAM, Doherty PJ, Williams DF. Molecular biointeractions of biomedical polymers with extracellular exudates and inflammatory cells and their effects on the biocompatibility *in vivo*. *Biomaterials* 1994;15:779–85.
- [38] Saad B, Neuenschwander P, Uhlenschmid GK, Suter UW. New versatile, elastomeric, degradable polymeric materials for medicine. *Intern J Biol Macromol* 1999;25:293–301.
- [39] Tracy MA, Ward KL, Firouzabadian L, Wang Y, Dong N, Qian R, et al. Factors affecting the degradation rate of poly(lactide-co-glycolide) microspheres *in vivo* and *in vitro*. *Biomaterials* 1999;20:1057–62.
- [40] Mukai K, Doi Y, Sema Y, Tomita K. Substrate specificities in hydrolysis of polyhydroxyalkanoates by microbial esterases. *Biotechnol Lett* 1993;15:601–4.
- [41] Malm T, Bowald S, Bylock A, Busch C, Saldeen T. Enlargement of the right ventricular outflow tract and the pulmonary artery with a new biodegradable patch in transannular position. *Eur Surg Res* 1994;26:298–308.



Fundamental Studies on Genetically Engineered Elastin Model Peptides for Biomaterials

Sachiro Kakinoki¹, Alyssa Panitch², David A. Tirrell³, and Tetsuji Yamaoka¹

¹Department of Biomedical Engineering, National Cardiovascular Center Research Institute, 5-7-1 Fujishirodai, Suita, Osaka 565-8565, Japan, ²Weldon School of Biomedical Engineering, Purdue University, IN 47907, USA, and ³Department of Chemical Engineering, California Institute of Technology, CA 91125, USA
e-mail: yamtet@ri.ncvc.go.jp

Elastin model peptide ((Val-Pro-Gly-Ile-Gly)₄₀; VPGIG₄₀) was designed and biosynthesized as injectable scaffold for cell transplantation therapies. In this report, the thermoresponsiveness and the potential as the base materials for injectable scaffold of VPGIG₄₀ expressed using genetic-engineering technique were explored.

Keywords: biomaterials, elastin model peptide, genetic engineering, injectable scaffold, thermoresponsiveness

Introduction

Recently, cell transplantation therapies are much attended with progress of regenerative medicine and stem-cell research. It is known that substantial effects can not be obtained only by injecting the cell suspensions and then feasible scaffolds are necessary for the cell transplantation therapies. Therefore, various biodegradable polymeric materials have been investigated as scaffolds actively. However, these scaffolds are not suitable for the cell transplantation therapy, because these bulk-type scaffolds require invasive surgery, and the cells inside the scaffold often necrotize. In order to solve these problems, photo-crosslinkable and thermoresponsible hydrogels have been investigated as injectable scaffolds. However, these non-biodegradable materials are not approved for the clinical use yet.

Elastin, the major component of elastic fibers in basement membrane, provides the resilience or restorative force to tissues. Noteworthy, soluble elastin-related polypeptides, such as tropoelastin, α -elastin and synthetic elastin model peptides, indicate the characteristics of temperature-depending phase transition. Therefore, we are interested in the potential of elastin model peptides as injectable scaffolds. In this report, we try to biosynthesize and characterize an elastin model peptide ((Val-Pro-Gly-Ile-Gly)₄₀; VPGIG₄₀) and develop the gel matrices consisting of VPGIG₄₀ to apply as injectable scaffold.

Results and Discussion

The elastin model peptides with repetitive sequence, VPGIG₄₀, were biosynthesized using *E. coli* [BL21(DE3)pLysS] which was transformed with an

expression-vector encoding VPGIG sequence [pET-28ap (VPGIG₄₀)] [1]. The insert region in pET-28ap (VPGIG₄₀) was confirmed by direct PCR of *E. coli* using primers which were flanking sequence of the insert region. By agarose electrophoresis, a band was observed at approximately 650 bp corresponding to the DNA length for the insert region of VPGIG₄₀. Protein expression was induced with the addition of β -isopropyl thiogalactoside (IPTG) and was allowed to continue for 24 hours. Protein purification was performed using the thermoresponsible property of VPGIG₄₀, namely, VPGIG₄₀ was purified with temperature control over/below the transition temperature. By SDS-PAGE, it is confirmed that crude VPGIG₄₀ was gradually purified by repeating this method and a clear band was indicated at approximately 18 kDa (Fig. 1). The purified VPGIG₄₀ was also confirmed by MALDI-TOF/MS analysis.

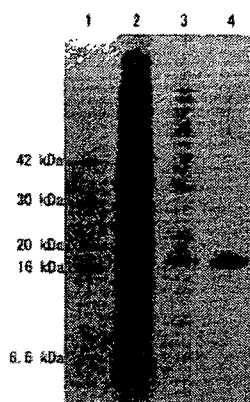


Fig. 1. SDS-PAGE (12%) for elastin model peptide VPGIG₄₀ at each purification step. (lane 1; marker, lane 2; bacterial lysate, lane 3; peptide purified once, lane 4; peptide purified twice)

Furthermore, the cloud points of purified VPGIG₄₀ were 28.2, 23.6 and 21.9 °C at 0.02, 0.05 and 0.1 w/v%, respectively. The mechanism for the temperature-depending phase transition of VPGIG₄₀ in solution has been suggested that the peptides are aggregated by hydrophobic interaction with conformational change from random-coil to β -spiral [2, 3].

The results suggest that genetically engineered VPGIG₄₀ has high potential as injectable scaffold for cell transplantation.

Acknowledgement

We are grateful to Prof. Shigeru Kunugi at Kyoto Institute of Technology.

References

1. Panitch, A., Yamaoka, T., Fournier, M. J., Mason, T. L., Tirrell, D. A. (1999) *Macromolecules*, **32**, 1701-1703.
2. Tamura, T., Yamaoka, T., Kunugi, S., Panitch, A., T., Tirrell, D. A. (2000) *Biomacromolecules*, **1**, 552-555.
3. Yamaoka, T., Tamura, T., Seto, Y., Tada, T., Kunugi, S., Tirrell, D. A. (2003) *Biomacromolecules*, **4**, 1680-1685.

マイクロ SPECT を用いた小動物イメージングの 定量的機能評価 Quantitative Functional Imaging of Small Animals Using MicroSPECT

銭谷 勉*
Tsutomu ZENIYA

要 旨

創薬や新規治療法の評価を目的とした前臨床研究において、小動物モデルを用いた *in vivo* イメージングは不可欠である。その中でも PET や SPECT などの高感度トレーサ技術である核医学的手法は生体内の生理機能を定量的に評価できるため大きな役割を果たしている。本論文では、小動物イメージングにおける定量的機能評価の意義および応用領域について言及した上で、マイクロ SPECT における動態解析および画像再構成の定量性について概論する。また、マイクロ SPECT を利用した定量的機能評価の例を紹介する。

キーワード：小動物、定量的機能評価、SPECT、ピンホールコリメータ、画像再構成

In vivo imaging of small laboratory animals facilitates objective assessment of pharmaceutical development and regenerative therapy in pre-clinical studies. Radionuclide imaging such as PET or SPECT is especially important because it allows to quantitatively assess physiological functions due to high sensitive tracing technique. This paper describes the significances and applications of quantitative functional assessment in small animal imaging, and then discusses quantitation about kinetic analysis and image reconstruction in microSPECT. Finally, it introduces quantitative functional imaging studies using microSPECT.

Key words: Small animal, Quantitative functional imaging, SPECT, Pinhole collimator, Image reconstruction

Med Imag Tech 26 (1): 14-20, 2008

1. はじめに

創薬や新規治療法を目的とした前臨床研究において、ラットやマウスなどの小動物モデルを用いた *in vivo* イメージングは不可欠である。また、近年の分子イメージング分野の発展に伴い、小動物専用の X 線 CT (Computed Tomography), MRI (Magnetic Resonance Imaging), PET (Positron Emission Tomography), SPECT (Single Photon Emission CT) および光イメージングなどの装置が盛んに開発されている。その中でも、PET や SPECT などの放射性同位元素をトレーサとして用いる核医学検査手法は、高い感度を有し、ト

レーサの集積の対して正確に比例した信号強度を提示するため、病態生理や病態生化学的な変化を定量的に評価することが可能であるため重要な役割を果たしている。

PET 装置は高い感度を有するが、高解像度の小動物用 PET 装置でもその空間解像度は 1 mm を超えておらず [1], 小病変の画像化に不十分である。PET は放射線同位元素から放出される陽電子が電子と結合する際に反対方向に放出される 2 本の消滅放射線をリング状の検出器で同時計測することで、放射線同位元素の存在する位置を推定する。陽電子が静止するまでの距離を陽電子の飛程と呼ぶが、核種によっては飛程が装置の空間解像度よりも大きく、解像度を悪化させる。たとえば、 ^{15}O の場合、陽電子のエネルギーが高く、陽電子が消滅するまでに水中で平均 2.5 mm 移動する。また、PET 核種は半減期が短いいため、小動物実験において、同一の個体の

* 国立循環器病センター研究所先進医工学センター
放射線医学部 [〒 565-8565 大阪府吹田市藤白台 5-7-1] : National Cardiovascular Center Research Institute.
e-mail: zeniya@ri.ncvc.go.jp
論文受付 : 2007 年 12 月 25 日
最終稿受付 : 2008 年 1 月 7 日

繰り返し撮像が行いやすいという利点である反面、サイクロトロンや放射性薬剤合成装置などの大掛かりな設備を必要とする。一方、SPECT装置は放射線同位元素から放出されるガンマ線の飛来方向を特定するためのコリメータを必要とするため、コリメータを必要としないPETに比べ感度が劣るのは避けられないが、コリメータの工夫次第ではPETよりも高い空間解像度が得られる。ピンホールコリメータは対象物がコリメータに近いほど感度および空間解像度を高くできるので (Fig. 1), 小動物イメージングに適しており, 1 mm 以下の解像度が比較的容易に実現できる [2, 3]. ほとんどの小動物用 SPECT 装置 (マイクロ SPECT) ではこのピンホールコリメータを利用している。感度が低いという問題は、複数のピンホールを利用することで克服する試みが行われている [4~6]. また, Table 1 に示されているように SPECT 検査で使用される放射性核種は半減期が長いので, PET では観測できない, 長時間における薬剤の動態を観察した

いという場合に適している。そして, 何よりも放射性薬剤を他施設から入手できるため, 安価で手軽に検査が実施できるという大きな利点がある。

従来のピンホール SPECT は, 体軸方向に画像が歪み, 視野内の解像度が不均一になるという問題があったため, 定量評価が困難であった。著者らは, この原因をデータの不完全性によるものと仮説をたて, 撮像軌道をラドン変換の完全性を満たすように設計し, 立体的な画像再構成理論を導入することで, 歪みのない視野全体で均一な解像度を有する 3 次元画像を得ることに成功した [7]. その結果, ピンホール SPECT においても小動物 PET 同様に定量評価が可能になった。しかしながら, PET や SPECT が得意とする, 定量的な機能評価をマイクロ SPECT で行う試みは, それほど広くなされていない。

本論文では, 小動物イメージングにおける定量的機能評価に必要とされる著者らの物理工学的な最近の進歩について述べる。最初に, 小動物イメージングの定量的機能評価の意義および応用領域について言及した上で, マイクロ SPECT における動態解析および画像再構成の定量性について概論する。最後に, 著者らが開発したマイクロ SPECT 装置を利用した定量的機能評価の例を紹介する。

2. 小動物イメージングにおける定量的機能評価の意義と応用領域

通常, 遺伝子改変や病態モデル動物はマウスやラットなどの小動物に対して行われており, 生きたまま, 小動物内の分子をイメージングする技術は非常に重要である。とくに, ヒトから実

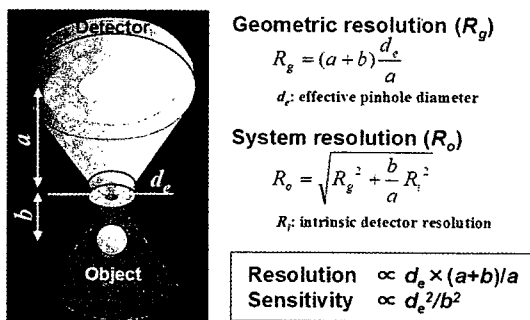


Fig. 1 Physics of pinhole SPECT. Spatial resolution and sensitivity can be improved by positioning a collimator closer to an object.

Table 1 Representative radionuclides used in SPECT study.

Isotope	Energy	Half life	Tracer	Application
^{99m}Tc	140 keV	6.01 hr	MDP/HMDP	bone scan
			MIBI	myocardial perfusion
			tetrofosmin	myocardial perfusion
			TRODAT	dopamine transporter
^{201}Tl	70 keV	72.9 hr	TlCl	myocardial perfusion
^{123}I	159 keV	13.3 hr	BMIPP	beta-oxidation
			MIBG	sympathetic
			β -CIT	dopamine transporter
			Iomazenil	benzodiazepine receptor
^{131}I	364 keV	8.04 day		thyroid
^{67}Ga	93, 185, 300 keV	3.26 day	citrate	tumor

験小動物まで同じ手技で定量的機能評価が可能な核医学イメージング技術は、血流などの生理的機能から種々の受容体、遺伝子発現、ペプチド・タンパクなどの疾患関連物質の体内動態までを観察できるため、創薬の迅速化・低コスト化や、テーラーメイド医療、遺伝子治療、再生医療などに代表される新しい病気の診断・治療法の開発に大きく貢献するといわれている。

創薬においては、治療化合物の探索から体内吸収・体内動態の評価、臨床試験早期に必要な毒性と薬効評価、投与量の最適化などの分野においての利用が開始されている。再生医療分野においても、多くの局面で本質的な情報を提示し、有効な治療法の確立に向けて重要な役割を果たすことは明らかである。たとえば、心筋梗塞部位での血管新生治療、細胞移植治療では、細胞の定着や血管の発達などの形態的な再生だけでなく、生体の一部の組織として機能評価を行うことが必要である。定着した細胞および組織の血流がどの程度回復し、種々の生理的な負荷などによって本来持つべき反応力（血流の自動調節能と血管反応性、代謝の制御、神経連絡過程など）をどの程度有し、必要な生体フィードバックを可視化できることが望ましい。これらの分野の基盤技術を整備するためには、疾患の本質を理解すること、そのための基礎、前臨床、および臨床研究を並行して実施すること、また、本質的な治療実施のための各種基盤技術を有していることが不可欠である。

3. マイクロ SPECT による定量的機能評価の問題点

SPECT データから、血流量、結合能などの定量的な生理パラメータを得るためには、コンパートメントモデル解析やグラフ解析など、トレーサの動態解析を行う必要がある [8]。このとき、入力関数と呼ばれる動脈中の放射能濃度の投与時からの時間変化が必要となる。ヒトの場合、通常、腕の動脈に穿刺し、撮像中にマニュアルで頻回採血やポンプを用いた連続採血を行って入力関数を得る [9]。ラットやマウスの血液量は、ヒトに比べて少量のため、採血量が多くなると貧血を起し、生理状態も大きく変化する。そのため、最低限の採血量に抑える必要があり、動脈と静脈を短絡させる arteriovenous (AV) シヤ

ント術を施し、そこから入力関数を得る方法が提案されている。

心筋機能の定量では、撮像された左心室から入力関数を得る方法が用いられる。しかし、これらの方法で得られる入力関数はあくまでも全血の放射能濃度であり、放射性薬剤が体内で代謝される場合、代謝産物の定量も行う必要もある。微量の血液中の代謝産物の定量は非常に困難である。このため、あらかじめ複数の同一動物で測定した平均入力関数を用いる方法や、入力関数の代わりにリファレンス領域を用いる方法 [10] がしばしば使われる。

得られたパラメータを解釈する際には、ヒトとの違いを考慮する必要がある。代謝速度はヒトと小動物では大きく異なる。通常、小動物の撮像は麻酔下で行われるが、麻酔の影響も無視できない。著者らは覚醒下に適したラット専用のホルダーを作製し、1 週間の馴化を行うことによって、覚醒下でのラット心筋血流量測定および血管反応性の評価を可能にした。

4. マイクロ SPECT 画像再構成における定量性

前述のようなトレーサの動態解析を行う場合、SPECT 画像の定量性が確保されていることが前提である。マイクロ SPECT 画像再構成においても、定量性を劣化させる要因を十分に考慮する必要がある。

1) 部分容積効果

核医学装置は、定量性が高いとしばしばいわれるが、部分容積効果（小さい対象物を空間解像度の悪い装置で撮像したとき発生する測定値の過小評価）は大きく定量性に影響する。とくに、小動物の場合サイズがヒトより小さいため、相応の高い空間解像度が要求される。たとえば、臨床で利用されている PET 装置は 5 mm 程度の空間解像度を持つが、この装置で得られた画像と同等の解像度でラットを撮像したければ 0.6 mm、マウスでは 0.4 mm の空間解像度が要求される [1]。実際の小動物用 PET の空間解像度は 1 ~ 2 mm 程度であるため、部分容積効果は小動物 PET ではヒトよりも大きな問題となる。これに対して、小動物用のピンホール SPECT では数百 μm の空間解像度を実現できるため、部分容積効果を抑制できる点で優位である。しかしなが

ら、部分容積効果の定量性に与える影響は少ないため、定量する際は十分に考慮する必要がある。コリメータ開口補正技術 [11] などを用いて解像度を改善するのも1つの方策である。

2) 吸収・散乱

SPECT で定量性を劣化させる大きな要因として、被写体内でのガンマ線の吸収および散乱がある。一般的な臨床脳 SPECT 検査では、60 ~ 80% の光子が体内での吸収を受け、30 ~ 40% の光子が散乱によって偽りの信号を与える。これらの影響を補正しなければ定量評価は難しい。飯田らは、実用的な手法によって吸収・散乱の影響を高い精度で補正することに成功し、SPECT でも PET 同様の定量評価を可能にした [12]。しかしながら、体内での吸収・散乱の影響は被写体の大きさに依存することを考えると、小動物ではヒトの場合に比べてそれほど大きくないと考えられる。Wang らはマウスにおける吸収・散乱の影響を、シミュレーションおよびファントム実験にて評価した。吸収も散乱も補正しない場合、15% 過小評価し、吸収補正のみ行った場合、9% 過大評価する。吸収と散乱の両方を補正して誤差は3%以下にできると報告している [13]。Deloar らは散乱線の影響に加え、ピンホールコリメータを突き抜けるガンマ線の影響も考慮する必要があることをシミュレーションによって示している [14]。この突き抜けガンマ線の影響はピンホール形状を knife-edge 型に代えて、keel-edge (channel-edge と呼ぶ) 型を使用することで抑制することができる [15]。

3) データの完全性

ピンホールコリメータを用いた SPECT 装置は原理上、3次元収集を行っているが、コーンビーム型の3次元画像再構成法が必要となる。ピンホール SPECT において単一の円軌道でデータを収集した場合、体軸方向に画像が歪み、空間解像度が不均一となるため、定量解析は困難である。画像再構成法を解析的手法の FBP (Filtered Back-Projection) に代えて、OSEM (Ordered Subsets Expectation Maximization) などの統計学に基づいた逐次近似画像再構成法を使用することによって改善されるが、視野周辺では依然として解像度の劣化は残っている [16]。最近の研究で、著者らはこの原因をデータの不完全性に起因するものと仮説をたて、撮像軌道をラドン変換の完全性を満たすような複数回転軸軌道とし、これに立体的画像再構成理論を導入することで、視野内で均一な高解像度を得ることに成功した (Fig. 2) [7]。Metzler らはヘリカル軌道で完全データ収集を実現している [17]。従来は定性的な評価のみに利用されてきた高解像度撮像法のピンホール SPECT だが、この問題の解決によって PET 同様に定量解析が可能になった。

4) トランケーション

ピンホールコリメータは対象物がコリメータに近いほど感度および解像度を高くできるのが特長であるが、極端に近づけるとトランケーション (データの欠損) が生じ、再構成画像のカウントは過大評価され、定量評価の妨げとなる。通常は被写体が視野から外れないように、被写

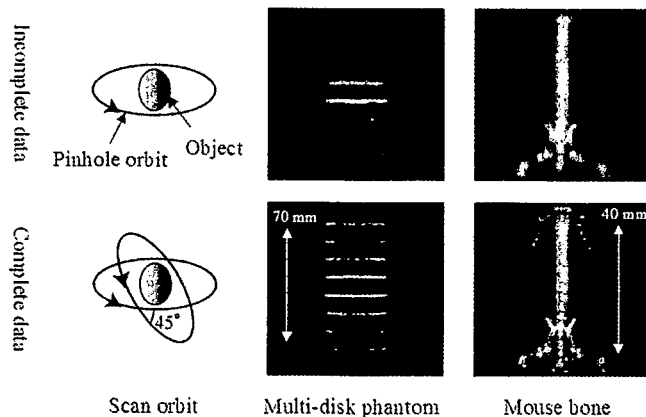


Fig. 2 Comparison between conventional acquisition and complete data acquisition in multi-disk phantom study and mouse bone scan with ^{99m}Tc. Data acquired by conventional single circular orbit are incomplete. Complete data are acquired by two-circular orbit. Complete data improve axial blurring and non-uniform spatial resolution in pinhole SPECT.